J. Membrane Biol. 145, 129–141 (1995)

The Journal of
Membrane
Biology

© Springer-Verlag New York Inc. 1995

Cellular Chloride Depletion Inhibits cAMP-activated Electrogenic Chloride Fluxes in HT29-18-C_1 Cells

D.M. Fine, C.F. Lo, L. Aguillar, D.L. Blackmon, M.H. Montrose
Departments of Medicine and Physiology, Johns Hopkins University School of Medicine, 720 Rutland Ave. Baltimore, MD 21205

Received: 14 June 1994/Revised: 27 January 1995

Abstract. Cyclic AMP-activated chloride fluxes have been analyzed in HT29-18-C_1 cells (a clonal cell line derived from a human colon carcinoma) using measurements of cell volume (electronic cell sizing), cell chloride content (chloride titrator) and intracellular chloride activity (6-methoxy-N-(3-sulfopropyl)quinolinium; SPQ). HT29-18-C_1 was shown to mediate polarized chloride transport. In unstimulated cells, the apical membrane was impermeable to chloride and net chloride flux was mediated by basolateral furosemide-sensitive transport. Forskolin (10 μM) increased furosemide-insensitive chloride permeability of the apical membrane, and decreased steady-state intracellular chloride concentration approximately 9%. Cellular chloride depletion (substitution of medium chloride by nitrate or gluconate), caused greater than fourfold reduction in cellular chloride concentration. When chloride-depleted cells were returned to normal medium, cells regained chloride and osmolytes via bumetanide-sensitive transport, but forskolin did not stimulate bumetanide-insensitive chloride uptake. The inhibition of cAMP-activated chloride reuptake was not explained by limiting cation conductance, cell shrinkage, choice of substitute anion, or decreased generation of cAMP in chloride-depleted cells. When cells with normal chloride content were depolarized (135 mM medium potassium + 10 μM valinomycin), cAMP activated electrogenic chloride uptake permselective for $Cl^- \approx Br^- > NO_3^- > I^-$. The electrogenic transport pathway was inhibited in chloride-depleted cells. Results suggest that chloride depletion limits activation of electrogenic chloride flux.

Key words: Cyclic AMP — Intestine — Secretion — Cell volume — Cellular chloride content

Correspondence to: M.H. Montrose

Introduction

The intestinal epithelium mediates electrogenic Cl^- secretion in response to elevation of intracellular second messengers, including cyclic AMP (cAMP) and calcium (Ca^{2+}) [15]. Disorders of chloride secretion are the basis for several diseases. Inappropriate stimulation of chloride secretion causes tissue water loss in diarrheal diseases [15]. Conversely, cystic fibrosis patients have lost the ability to stimulate intestinal chloride secretion in response to cAMP/PKA [10, 35] and Ca^{2+}/PKC [19, 35] second messenger pathways. Study of cells from cystic fibrosis patients has identified tissue-specific regulation of chloride secretion, because cystic fibrosis airway epithelia can still mediate chloride secretion in response to calcium mobilizing agonists [22, 45].

The basis for tissue-specific regulation of chloride secretion remains uncertain. Based on observations that the cystic fibrosis gene product (CFTR) can function as a small conductance ohmic chloride channel activated by cAMP/PKA [3, 2, 7] or Ca^{2+}/PKC [9, 14], one simple explanation is that CFTR is the main route for intestinal Cl^- secretion, whereas airway cells express additional chloride channels besides CFTR [3]. In support of this model, a diversity of epithelial chloride channels have been observed in both normal and CF tissue [40], including Ca^{2+}-activated chloride channels in airway cells [5].

Observations suggest that regulation of intestinal chloride secretion is more complex than suggested by this simple model. Multiple chloride channel types have been identified in intestinal epithelial cells based either on molecular cloning (ClC-2), or patch clamp analyses [5, 13, 41]. In addition, endogenous CFTR expression has not always correlated with the observation of cAMP-stimulated chloride fluxes or the appearance of the ohmic chloride channel in HT29 intestinal cells [31, 32, 33]. Finally, regulation of membrane recycling and cytoskeleton have been shown to affect the activity and/or dis-

tribution of both apical chloride channels and basolateral Na/K/Cl cotransport proteins in intestinal cells [11, 28, 36].

Recent evidence suggests that intracellular chloride may also contribute to regulation of membrane transport and/or plasma membrane recycling. It has been shown that lowered intracellular chloride concentration is required to activate multiple sodium transporters in parotid acinar cells [37]. Conversely, cellular chloride depletion inhibits protein secretory pathways in neutrophils [17] and inhibits cAMP-stimulated endocytosis in intestinal T84 cells [36]. Chloride depletion also inhibits CFTR internalization in T84 cells, and affects CFTR channel activation in LTK-fibroblasts heterologously expressing CFTR [36, 44]. Based on these results, we questioned whether chloride depletion affected cAMP-stimulated chloride flux routes in a model intestinal epithelia. The HT29 model has been used previously to identify factors required for expression of CFTR [30, 31] and cAMP-activated chloride channels [32, 33]. Here we characterize cAMP-activated chloride flux routes in a stably differentiated HT29 subclone (HT29-18-C_1) [15, 31], and report that activation of electrogenic cAMP-stimulated chloride fluxes is inhibited by intracellular chloride depletion.

Materials and Methods

Cell Culture

HT29-18-C_1 cells obtained from Daniel Louvard (Institut Pasteur, Paris, France) were used 8–18 passages after cloning from the parent line [20]. For simplicity, the cells will be referred to as HT29-18-C_1 cells. Cells were cultured in Dulbecco's modified Eagle's medium containing 25 mM glucose and supplemented with 10 mg/ml human transferrin (Sigma), 50 IU/ml streptomycin, 50 mg/ml penicillin, 4 mM glutamine, and 10% fetal calf serum. Cells were grown at 37°C in humidified 10% CO_2/90% air in plastic flasks (Costar, Cambridge, Mass), with culture medium changed daily [31].

Solutions

All media were approximately 310 mosmol/kg H_2O as measured on a Wescor 5500 vapor pressure osmometer (Logan, UT). All experiments were performed using solutions equilibrated with room air at 37°C. Chloride medium contained (in mM): 130 NaCl, 5 KCl, 2 $CaCl_2$, 20 HEPES, 1 $MgSO_4$, 0.83 Na_2HPO_4, 0.17 NaH_2PO_4, 25 Mannose, titrated to pH 7.4 with NaOH. Compared to chloride medium, gluconate medium had gluconate salts substituted mol:mol for all chloride salts, nitrate medium had nitrate salts substituted mol:mol for all chloride salts, and potassium medium substituted KCl mol:mol for NaCl. All other experimental solutions are described in the text or below.

Electronic Cell Sizing

Cells in flasks were trypsinized into a single cell suspension as described [38]. Routinely, suspended cells were allowed to reequilibrate in chloride medium for 60 to 120 min with gentle mixing at 37°C prior to experimental use. To preincubate cells in different media, trypsinized cells were aliquotted into 2 ml microfuge tubes, centrifuged ($2000 \times g \times 10$ sec) and the cell pellet resuspended in medium of the desired composition (e.g., chloride gluconate, or nitrate medium). The volume of suspended HT29-C_1 cells was measured at 37°C with a Coulter Counter (Model ZM, Hialeah, FL) coupled to a computerized (CompuAdd 286/12, Austin, TX) pulse height analyzer (Tennelec/The Nucleus, Oak Ridge, TN) as described previously [38]. Briefly, 1 ml of cell suspension was injected into 25 ml experimental medium at time zero, and cell volume was measured at subsequent time points. Each measurement represents averaged data from 15,000 to 35,000 cells collected over 8 sec. Using histograms of cell number *vs.* single cell volume, the computer automatically determined the centroid of the single cell volume distribution in femtoliters (10^{-15} liters, equivalent to μm^3). The instrument was calibrated using latex beads of known volume (Coulter).

Cellular Chloride Content

Intracellular chloride content was determined using a chloride titrator as described [38]. Briefly, cells on 35 mm dishes were preincubated for 60 min with chloride, gluconate, or nitrate medium (as described in figure legends) and then immersed in experimental media for the time noted in figures. For chloride determination, cells were washed three times in an ice-cold Cl-free medium (in mM): 130 TMA-NO_3, 1 $MgSO_4$, 10 HEPES, 2 EGTA, pH 7.4, lysed in 10% perchloric acid, and ion content measured with a Labconco Digital Chloridometer (calibrated with standards in 10% perchloric acid). Results were normalized to cellular protein [12], with bovine gamma globulin as standard.

Chloride Efflux

Efflux of isotopic chloride was measured precisely as described previously [31]. Briefly, cells on 35 mm plastic dishes were preequilibrated two hours with 4 μCi/ml ^{36}Cl in chloride medium, washed with ice-cold gluconate medium, and then at time zero exposed to 37°C gluconate medium to initiate efflux. As performed previously, some cells were exposed to 1 μM ionomycin (Calbiochem) at time zero, or 10 μM forskolin (Calbiochem) in the last 5 min of isotopic preequilibration. Twelve time points were collected in the first 15 min of efflux, and results presented as the efflux rate constant after fitting the data to a single exponential [31].

Qualitative Measurements of Cell Chloride Activity

HT29-C_1 cells were grown on permeable filter supports (Anotec) as described previously [29, 39]. Confluent cells on filters were loaded with the chloride sensitive fluorescent dye 6-methoxy-N-(3-sulfopropyl)quinolinium inner salt (SPQ: Molecular Probes, OR) [21] by overnight incubation with 10–20 mM SPQ added to culture medium. Filters with dye-loaded cells were mounted in a chamber allowing separate apical and basolateral perfusion [29], and studied on the stage of a digital imaging microscope [39]. Cellular fluorescence was excited at 380 ± 10 nm, and emission monitored at 510 ± 40 nm with a Hamamatsu intensified CCD camera (Model C2400-97) operating at constant intensifier gain and constant camera gain. Data were collected as digitized 4-frame averages (128 msec/image) by a Perceptics image processor (Knoxville, TN). In each experiment, 20 cells in the camera field were selected for real-time analysis. During an experiment, the

average pixel intensity in each selected cell (116 pixels/cell = 15 μm^2) was calculated separately within each collected image, and camera background values were subtracted from fluorescence values. To compile the fluorescence response from multiple cells, the fluorescence of each cell was normalized to its initial fluorescence at the start of the experiment. Results from a single experiment are presented as average normalized values from all cells selected for real-time analysis. Calibrations of SPQ *vs.* intracellular chloride concentration were not considered reliable because of (i) our inability to fully deplete cells of intracellular chloride (*see results*), and (ii) dye leakage (*data not shown*).

Cyclic AMP Assay

Intracellular cAMP levels were assayed using a titrated cyclic AMP radioimmunoassay (Amersham, Arlington Heights, IL). HT29-C_1 cells on 35 mm dishes were experimentally treated, washed three times in ice-cold gluconate medium, and then lysed in 1 ml ice-cold 0.6N perchloric acid for at least 5 min. Aliquots (950 μl) of lysate were transferred to a microfuge tube, pH neutralized with (85 μl) 5M K_2CO_3, samples vortexed, then centrifuged (16,000 × g × 5 min). Aliquots (50 μl) of the supernatant were assayed for cAMP as described by the manufacturer (Amersham, Arlington Heights, IL). Results were normalized to cellular protein.

Miscellaneous

Unless otherwise indicated, all chemicals were obtained from Sigma or Fluka and were of the highest grade available. HEPES was obtained from Research Organics. Bumetanide was the generous gift of Hoffman-LaRoche. Furosemide was the generous gift of Hoechst-Roussel Pharmaceuticals. Statistical significance was determined using one-way analysis of variance (ANOVA) or unpaired two-tailed *t*-test. Average values are presented as mean ± SEM.

Results

Results of initial experiments suggested that increasing cellular cAMP caused net osmolyte loss from HT29-C_1 cells. As shown in Fig. 1, HT29-C_1 cells shrink when exposed to the cAMP agonist forskolin, but not the inactive derivative 1,9-dideoxyforskolin [43]. In three preparations, a statistically significant shrinkage was observed after 10 min incubation in forskolin (74 ± 7 fl, $P < 0.01$ compared to cells without drug), but not 1,9-dideoxyforskolin (11 ± 6 fl, $P > 0.05$).

Activation of Chloride Uptake and Chloride Efflux Mechanisms by cAMP

Isotopic chloride efflux was used to define the presence of cAMP-stimulated chloride transport mechanisms in HT29-C_1. As shown in Fig. 2, either forskolin or calcium ionophore (1 μM ionomycin) stimulated ^{36}Cl efflux into chloride-free medium (gluconate substitution). In four experiments, the rate constant of net chloride efflux from unstimulated cells (0.29 ± 0.05 min^{-1}) was significantly increased by either forskolin or ionomycin (0.67 ± 0.02 min^{-1} or 0.75 ± 0.16 min^{-1}, respectively; both conditions $P < 0.05$ *vs.* untreated cells by ANOVA). Thus, the stably differentiated HT29-C_1 cell is a suitable model to study cAMP-activated chloride fluxes, unlike the HT29-18 parent line which fails to demonstrate

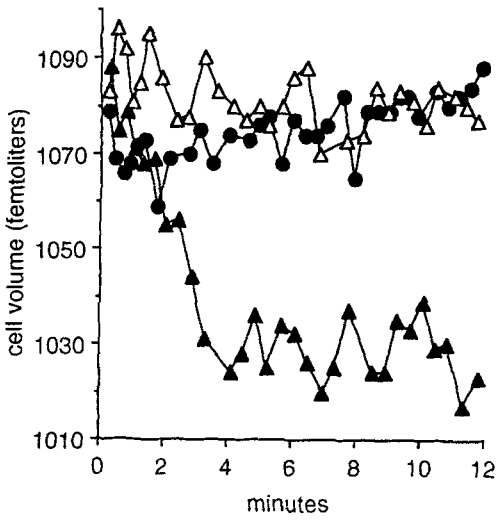

Fig. 1. Effect of cAMP on cell volume of HT29-C_1 cells. Suspended HT29-C_1 cells were equilibrated at 37°C for 1 hr in chloride medium. At time zero, a 1 ml aliquot of cells was injected into 25 ml of chloride medium (●), chloride medium containing 10 μM forskolin (▲) or 10 μM 1,9-dideoxyforskolin (△) as hydrophobic control. Cell volume was measured as the indicated times by electronic cell sizing, and results are presented as the mean single cell volume in the population. Results of a single representative experiment are shown. Compiled results from three experiments are presented in results.

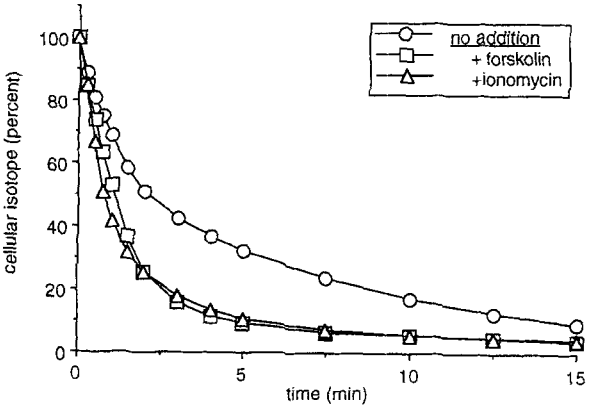

Fig. 2. Effect of forskolin or ionomycin on net isotopic chloride efflux. Cells were pre-equilibrated 2 hr with 4 μCi/ml ^{36}Cl added to chloride medium. At time zero, cells were exposed to gluconate medium and samples collected at the indicated time points. When required, cells were exposed to 10 μM forskolin (□) 5 min prior to initiating efflux, or 1 μM ionomycin (△) at time zero. Results were analyzed as described in Materials and Methods [26]. Results from a single representative experiment are shown. Compiled results from four experiments are presented in results.

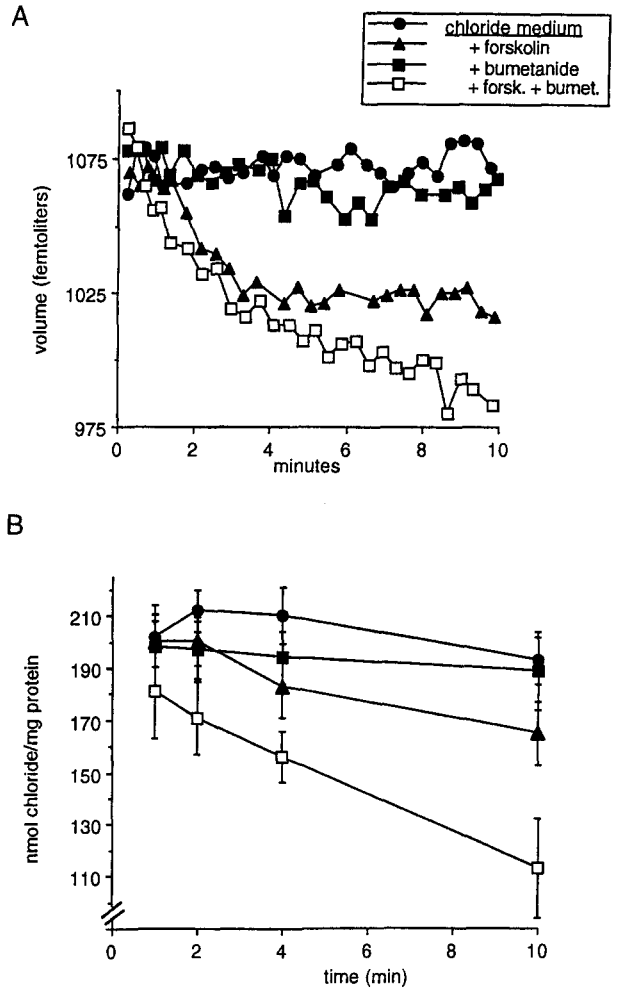

Fig. 3. Effect of forskolin and bumetanide on cell volume and cell chloride content. At time zero, cells pre-equilibrated in chloride medium were exposed to the same medium (●), or chloride medium containing 100 μM bumetanide (■), 10 μM forskolin (▲), or both drugs (□). (*A*) Cell volume of suspended HT29-C_1 cells was measured as described in Fig. 1 and Materials and Methods. Results from a single representative experiment are shown in the figure. Compiled results from five experiments are presented in results. (*B*) At the indicated times, cells on plastic dishes were processed for measurement of cell chloride content. HT29-C_1 cell extracts were measured using a chloride titrator as described in Materials and Methods. Results in *B* are mean ± SEM of five observations.

cAMP activated chloride fluxes in either the undifferentiated or differentiated state [31].

Measurements of cell volume and cell chloride content were used to test whether cAMP changed net ion content when chloride was kept constant in the medium. As shown in Fig. 3*A*, the volume of unstimulated cells was not significantly affected by 10 min exposure to 100 μM bumetanide (an inhibitor of Na/K/2Cl cotransport [27, 28] (7 ± 8 fl shrinkage observed in five preparations). Over the same time course, bumetanide had a larger effect in cells simultaneously exposed to forskolin (32 ± 8 fl, $P = 0.02$ *vs.* effect of bumetanide alone in paired measurements). This suggests the forskolin activated net osmolyte uptake via a bumetanide-sensitive transporter. Qualitatively similar results were observed with 1 mM furosemide, another inhibitor of Na/K/2Cl cotransport (*data not shown*). The effect of bumetanide was corroborated by measurements of cellular chloride, shown in Fig. 3*B*. The chloride titrator assay confirmed that bumetanide-sensitive chloride efflux (net loss of 2 ± 10 nmol Cl^-/mg protein after 10 min drug exposure, n = 5 experiments) was significantly larger ($P = 0.002$) in the presence of forskolin (56 ± 7 nmol Cl^-/mg protein, n = 5 experiments).

As described below, the magnitude of forskolin-sensitive chloride loss suggests that cAMP also activates a net chloride efflux pathway which is bumetanide-insensitive. Forskolin causes a 5.4 ± 0.8 percent cell shrinkage (10 min time point, n = 5 preparations). If cell chloride redistributed passively with this reduced cell water content (i.e., if the final intracellular [Cl^-] was the same in forskolin-treated cells), a 5% decrease of cell chloride content should be observed. However, a 14 ± 2 percent decrease was observed (n = 9). In the presence of bumetanide, an even larger discrepancy was noted between the predicted effects of forskolin on passive chloride loss (8%) *vs.* the observed loss of 41 ± 13 percent cell chloride (n = 3). These results strongly suggest that intracellular chloride concentration decreases after forskolin exposure, despite cAMP activation of chloride uptake via bumetanide-sensitive transport. These results are most easily explained by cAMP activation of a bumetanide-insensitive chloride efflux mechanism.

Polarity of Chloride Fluxes in Resting and cAMP-stimulated HT29-C_1 Cells

Confluent cells grown on membrane filters were loaded with a chloride-sensitive indicator dye (SPQ) [21] and studied in a chamber which allowed separate superfusion at the apical *vs.* basolateral surfaces [29, 39]. Experiments started after cells were preincubated in nitrate medium. As shown in Fig. 4, SPQ fluorescence was strongly quenched by addition of basolateral, but not apical, Cl^-. Subsequent removal of apical Cl^- also had no effect on SPQ fluorescence, even though addition of a strongly quenching anion (130 mM SCN) demonstrated that significant anion-sensitive fluorescence was still present. Since a decrease in SPQ fluorescence indicates increased cellular [Cl^-], results suggest that only the basolateral membrane is permeant to chloride in unstimulated HT29-C_1 cells. As shown in Fig. 5, basolateral chloride permeability was diminished by 1 mM furosemide, suggesting that basolateral Na/K/2Cl cotransport mediated chloride uptake across the basolateral membrane. The more potent inhibitor bumetanide could not be used in these experiments, because bumetanide fluorescence in the medium interfered with quantification of cellular SPQ fluorescence (*data not shown*).

As described below, results suggested that forskolin

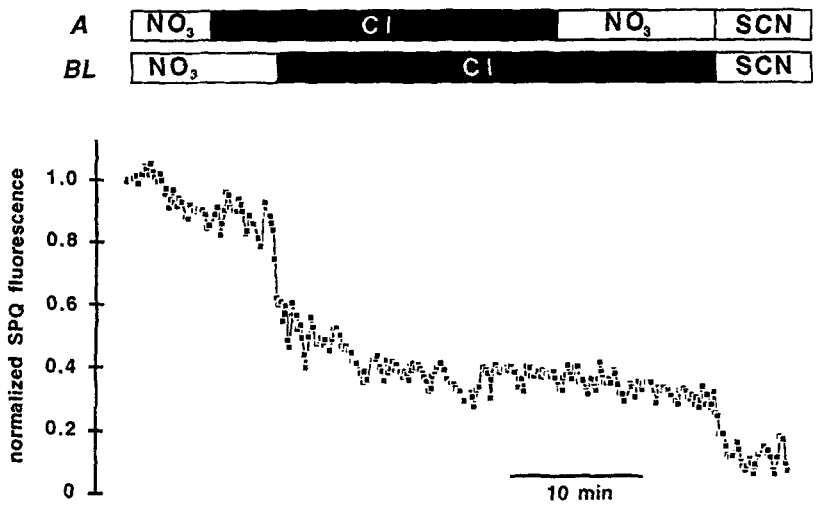

Fig. 4. Polarity of cell chloride permeability in HT29-C_1 cells. Cell monolayers grown on permeable filter supports were exposed overnight to 10 mM SPQ in culture medium. The following day, cells were preincubated in nitrate medium for 60 min prior to experimental use. Dye-loaded cells were mounted in a chamber which allowed independent perfusion of the apical (*A*) and basolateral (*BL*) cell surfaces [25], and fluorescence measured using a digital imaging microscope as described in Materials and Methods. During the experiment, cells were exposed to nitrate medium (NO_3), chloride medium (Cl) or medium in which 130 mM sodium thiocyanate replaced 130 mM NaCl in chloride medium (SCN). Results are the average fluorescence of 20 randomly selected cells in the monolayer, and are normalized (as described in Materials and Methods) to compensate for variability in dye loading between cells. Qualitatively similar results were observed in five experiments.

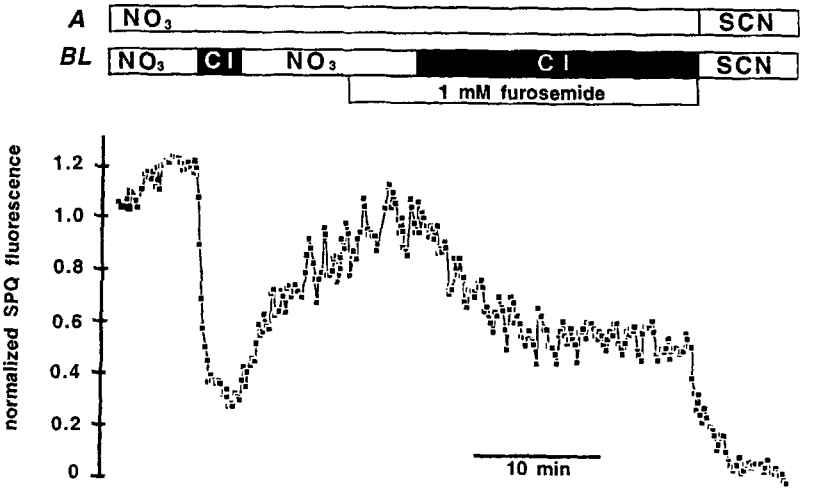

Fig. 5. Furosemide inhibits basolateral chloride permeability in HT29-C_1 cells. Monolayers of SPQ-loaded cells on filters were studied as described in Fig. 4. At the indicated times 1 mM furosemide was added to basolateral perfusates. Results are the average fluorescence of 20 randomly selected cells in the monolayer, and are normalized (as described in Materials and Methods) to compensate for variability in dye loading between cells. Qualitatively similar results were observed in three experiments.

increased an apical membrane chloride permeability which was furosemide-insensitive. As shown in Fig. 6, varying chloride concentrations in the apical superfusate caused larger changes in SPQ fluorescence after addition of forskolin. This suggests that cAMP increased apical membrane chloride permeability. In Fig. 7, the entire experiment was performed in the presence of 10 μM forskolin in all perfusates. In this condition, removal of apical chloride stimulated an increase of SPQ fluorescence (chloride efflux) which was not inhibited by addition of 1 mM furosemide to the apical perfusate.

Contribution of Chloride to Cell Volume: Effects of Medium Chloride Removal

Previous results suggested that cellular sodium and potassium were present at a total of ≈500 nmol/mg protein [38]. If these cations are assumed to contribute 130 mM to cellular contents, then values of total chloride content (214 ± 7 nmol/mg protein, n = 25) indicate a chloride concentration of 56 mM in unstimulated cells. Values of cell chloride content and cell volume from Fig. 2 estimate that intracellular [Cl] is reduced to 51 mM after 10 min forskolin stimulation, or 36 mM in the presence of bumetanide plus forskolin.

To establish the relationship between intracellular chloride content and cell volume, both parameters were measured in parallel during successive lowering of medium chloride (Fig. 8). As shown in Fig. 8*A*, net loss of cell chloride followed iso-osmotic substitution of medium chloride by either gluconate or nitrate. In the presence of either substitute anion, loss of cell chloride was correlated with cell shrinkage (Fig. 8*B*), but less shrinkage was observed in the presence of nitrate (presumably

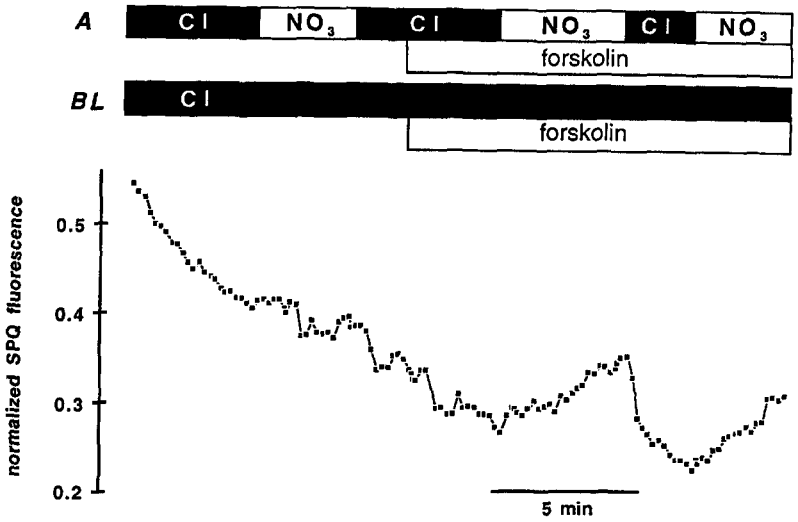

Fig. 6. Forskolin increases apical membrane chloride permeability in HT29-C_l cells. Monolayers of SPQ-loaded cells on filters were studied as described in Fig. 4. At the indicated times 10 μM forskolin was added to apical and basolateral perfusates. Results are the average fluorescence of 20 randomly selected cells in the monolayer, and are normalized (as described in Materials and Methods) to compensate for variability in dye loading between cells. Qualitatively similar results were observed in five experiments.

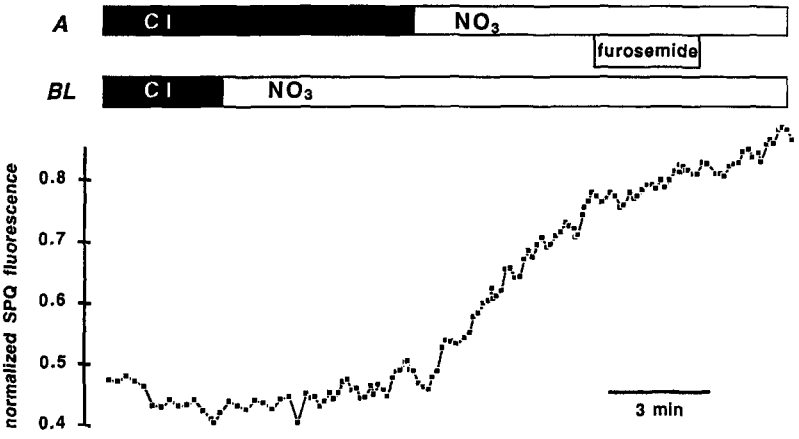

Fig. 7. Forskolin-stimulated apical membrane chloride permeability is insensitive to furosemide. Monolayers of SPQ-loaded cells on filters were studied as described in Fig. 4. Ten micromolar forskolin was present in all apical and basolateral perfusates. Results are the average fluorescence of 20 randomly selected cells in the monolayer, and are normalized (as described in Materials and Methods) to compensate for variability in dye loading between cells. At the indicated time, 1 mM furosemide was added to the apical perfusate. Similar results were observed in five experiments.

because entry of nitrate partially compensated for chloride loss). The decrease in chloride content and cell volume after one hour incubation in chloride-free media was used to calculate the residual chloride concentration; 13 mM in gluconate medium, 10 mM in nitrate medium.

Flame photometry measurements of cellular K^+ and Na^+ content [38] demonstrated that chloride depletion in gluconate medium did not greatly disturb cellular content of monovalent cations. The K^+ and Na^+ content of resting cells (475 ± 28 nmol K^+/mg protein and 26 ± 2 nmol Na^+/mg protein, n = 12) was only decreased slightly following 60–120 min in gluconate medium (to 436 ± 25 nmol K^+/mg protein and 22 ± 1 nmol Na^+/mg protein).

These experiments suggest that (i) cell chloride is a major determinant of cell volume, (ii) cell volume can be used as a sensitive indicator of intracellular Cl^- levels when gluconate is used as a substitute anion, and (iii) 60 min incubation in chloride-free medium depletes cells of 80% of cell chloride, and lowers intracellular chloride concentration at least fourfold.

Asymmetry of cAMP-activated, Bumetanide-insensitive Cl^- Fluxes

Following chloride depletion, cells regained normal volume when returned to chloride medium. As shown in Fig. 9*A*, bumetanide blocked this reswelling, suggesting that the Na/K/2Cl cotransporter was responsible for reuptake of osmolytes under these conditions. This was corroborated by measurements of bumetanide-sensitive chloride uptake during the reswelling phase (Fig. 9*B*). Combined with earlier experiments (Figs. 4 and 5), these results suggest that a major mechanism for chloride uptake in unstimulated cells is a basolateral bumetanide-sensitive transporter.

As shown in Fig. 9*B*, a slow bumetanide-insensitive chloride uptake was observed when chloride-depleted cells were reexposed to chloride, but this pathway was not affected by forskolin. In addition, there was no significant bumetanide-insensitive cell volume change stimulated by forskolin (Fig. 9*A*). These results were surpris-

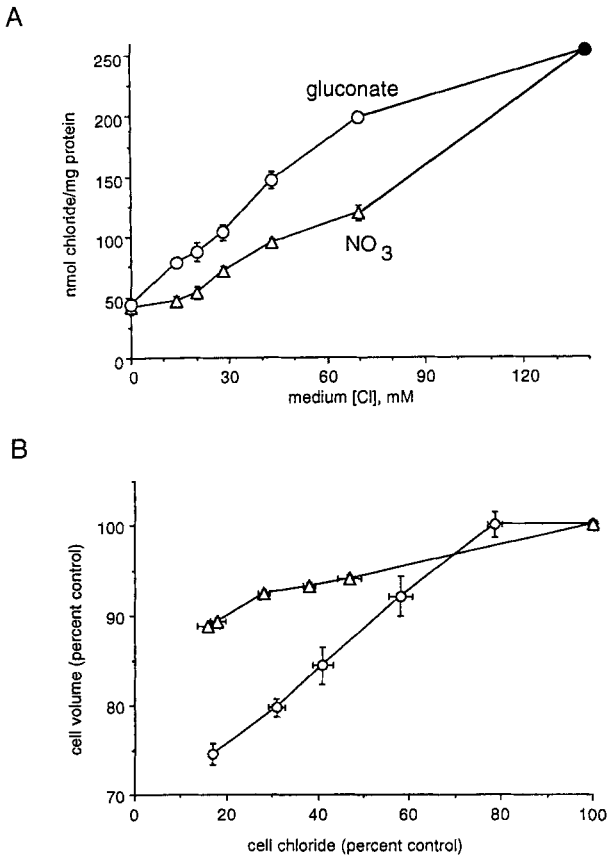

Fig. 8. Effect of medium anion substitution on cell chloride content and cell volume. HT29-C_1 cells (in suspension or on plastic dishes) were incubated 60 min at 37°C in chloride medium (●) or media in which the chloride had been replaced mol:mol either by NO_3 (△) or gluconate (○). At the end of the incubation, cell volume (suspensions) and cell chloride content (plastic dishes) was determined. Results are presented as the mean ± SEM of 4–6 measurements. (*A*) Intracellular chloride content is presented *vs.* the amount of chloride in the incubation medium. (*B*) Cell volume is plotted *vs.* cell chloride content. Results are normalized to the respective values of these parameters in chloride medium. Each symbol compiles results from a single concentration of medium chloride from the upper graph (with the exception that cell volume was not determined for 20 mM [Cl]). As shown, chloride depletion is correlated with cell shrinkage, but results differ based on choice of NO_3 *vs.* gluconate as a substitute anion.

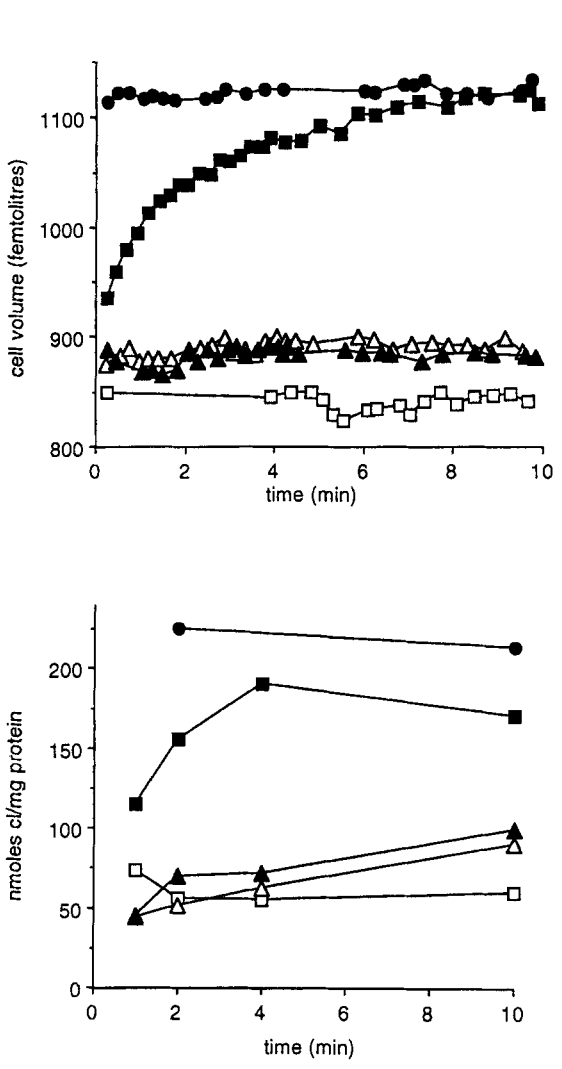

Fig. 9. Chloride-depleted cells regain both cell volume (*A*) and cell chloride (*B*) when returned to chloride medium. Control cells were preincubated in chloride medium and maintained in chloride medium at time zero (●). All other cells were Cl^--depleted by 60 min preincubation in gluconate medium. Some chloride-depleted cells were maintained in gluconate medium at time zero (□), whereas others were exposed to chloride medium (■, △, ▲). At time zero, some cells were additionally exposed to 10 μM forskolin (▲), and/or 100 μM bumetanide (△, ▲). Results from representative experiments are shown, but qualitatively similar results were observed in either five (*A*) or four (*B*) experiments.

ing because of prior observations in chloride-replete cells: of cAMP-stimulated, loop diuretic-insensitive net chloride efflux (Figs. 2, 3 and 6), and influx (Fig. 6). Using chloride-depleted cells, we had anticipated that forskolin would stimulate a large net chloride uptake due to the fourfold steepening of the inward chloride gradient caused by chloride depletion. Experiments were pursued to reconcile these observations.

Experiments tested different cAMP agonists, and verified the effects of forskolin on cellular cAMP levels in different conditions. No stimulation of bumetanide-insensitive chloride uptake or swelling was observed when chloride-depleted cells were exposed to 0.1 mM IBMX plus 10 μM forskolin, 0.1 mM dibutyryl cAMP, or 1 mM 8-Br-cAMP (*data not shown*). Further experiments verified that forskolin could elevate cAMP in chloride-depleted cells. The Table shows that cAMP levels were elevated similarly by forskolin in both chloride-replete and chloride-depleted cells. These results suggested that forskolin was an appropriate agonist in chloride-depleted cells, and that alternative means of stimulating the cAMP signal transduction pathway gave equivalent results.

Experiments were designed to test whether cell

Table 1. Intracellular cAMP levels in HT29-C_1 cells

Preincubation medium	Addition at t = 0	cAMP level at t = 1 min (pmol cAMP/mg protein)
Chloride		2.8 ± 0.5
Chloride	+ Forskolin	19.4 ± 0.7
Gluconate		2.1 ± 0.4
Gluconate	+ Forskolin	14 ± 2
Gluconate	Chloride + bumetanide	1.1 ± 0.1
Gluconate	Chloride + bumet + forskolin	27 ± 0.1

HT29-C1 cells on plastic coverslips were preincubated in either gluconate or chloride medium (as indicated) for 60 min. Following preincubation, medium was changed at time zero as indicated in the second column. At time zero, cells were either maintained in the same medium salts as during the preincubation, or switched from gluconate to chloride medium. In addition, some cells were exposed to 10 μM forskolin and/or 100μM bumetanide at time zero. After 1 min incubation, cells were processed for cAMP measurement via radioimmunoassay, as described in Materials and Methods. Results are presented as mean ± SEM of four observations.

shrinkage, or the use of gluconate as a substitute anion, inhibited the cAMP-stimulated bumetanide-insensitive Cl^- flux route. Cells preincubated in nitrate medium had equivalent chloride depletion *vs.* cells preincubated in gluconate, but nitrate-preincubated cells only shrink 10% (compare to 26% shrinkage after gluconate preincubation, *see* Fig. 8). As shown in Fig. 10*A*, nitrate-preincubated cells gave qualitatively similar results as gluconate-preincubated cells; there was no forskolin-stimulated, bumetanide-insensitive volume change when cells were returned to chloride medium. However, results were different when cells preincubated in chloride medium were rapidly shrunken to the same extent as nitrate-preincubated cells (by exposure to a hypertonic chloride medium supplemented with 40 mM sucrose). As shown in Fig. 10*B*, cells in hypertonic media continued to demonstrate forskolin-stimulated chloride efflux. These results suggest that the forskolin-stimulated, bumetanide-insensitive transport route could still function in shrunken cells.

Experiments were performed to test whether cation conductance limited chloride uptake into chloride-depleted cells. Neither increased sodium permeability (2 μM gramicidin D), nor increased potassium permeability (10 μM valinomycin) stimulated osmolyte uptake via the bumetanide-insensitive flux route (Fig. 11). In the presence of valinomycin, potassium efflux may compensate for chloride influx and cause volume change to be minimal, therefore parallel measurements of chloride reuptake were performed. In chloride-depleted cells exposed at time zero to forskolin and bumetanide in chloride medium, there was no difference in the rate of chloride reuptake in the absence *vs.* presence of valinomycin (6 ± 2 nmol chloride uptake/min/mg protein and 5 ± 2 nmol chloride uptake/min/mg protein, respectively; n = 5). These results suggest that cation conductance does not limit chloride flux.

Experiments were performed to test whether membrane potential limited chloride influx. We first studied depolarized cells with normal chloride content (chloride-replete cells), assuming that if we could demonstrate electrogenic chloride uptake, then cells depleted of chloride would have a larger driving force for net chloride entry (due to the fourfold larger inward chloride gradient) in the same medium. As shown in Figure 12*A*, when chloride-replete cells were exposed at time zero to high potassium (135 mM) and bumetanide in the medium we observed a slow swelling which was not affected by addition of valinomycin. In contrast, forskolin stimulated bumetanide-insensitive swelling which was further enhanced by addition of valinomycin. This suggests that forskolin activates an electrogenic, bumetanide-insensitive osmolyte uptake in chloride-replete cells.

Using a related depolarization protocol we determined the apparent permeability of several anions for the forskolin-stimulated flux route observed in Fig. 12*A*. Cells preequilibrated in chloride medium were added to different high potassium media (with valinomycin and bumetanide) in which 130 mM chloride was replaced mol:mol by Br^-, I^-, or NO_3^-. Volume was measured at the indicated time points, and results presented as the volume difference between the presence *vs.* absence of forskolin at each time point. Results were compared to the swelling observed when cells were incubated in standard potassium medium containing chloride as primary anion. A forskolin-stimulated volume decrease suggested that chloride loss was faster than uptake of an alternative anion from the medium. As shown in Fig. 13, the relative anion permeability of the forskolin-stimulated, bumetanide insensitive flux was $Cl^- \approx Br^- > NO_3^- > I^-$.

Results were different when the depolarization protocol was applied to chloride-depleted cells. As shown in Fig. 12*B*, forskolin-stimulated osmolyte uptake was negligible in early (< 20 min) time points, either in the presence or absence of valinomycin. However, signifi-

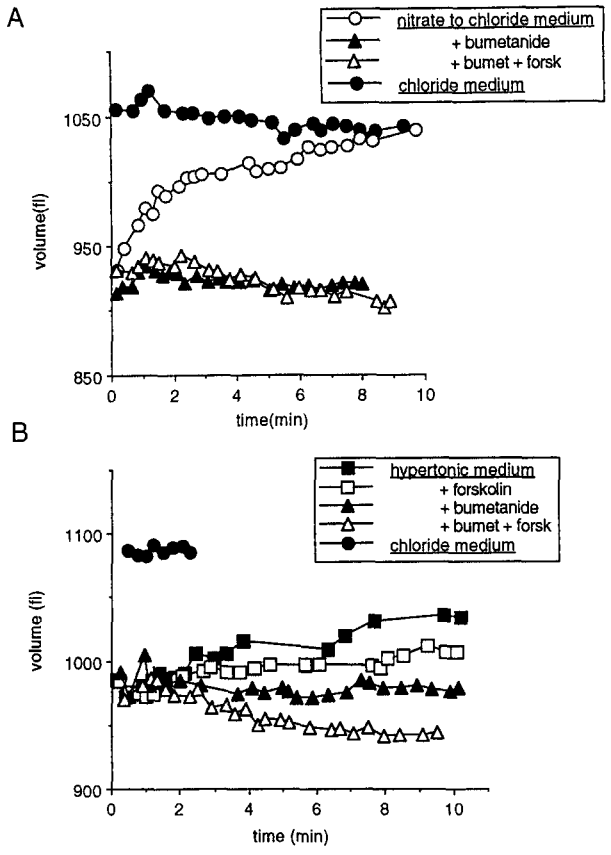

Fig. 10. Effect of anion substitution and cell shrinkage on cAMP activation of the bumetanide-insensitive osmolyte flux. Cell volume was followed *vs.* time as described in Fig. 1. Control cells were preincubated in chloride medium and maintained in chloride medium throughout the experiment (●). (*A*) Cells were Cl^--depleted by 60 min preincubation in nitrate medium. At time zero, Cl-depleted cells were returned to chloride medium (○, △, ▲). Some cells were additionally exposed at time zero to 10 μM forskolin (▲) and/or 100 μM bumetanide (△, ▲). (*B*) At time zero, cells preincubated in chloride medium were exposed to hypertonic medium (chloride medium plus 40 mM sucrose) (□, △, ■, ▲). Some cells were additionally exposed to 10 μM forskolin (□, △) and/or 100 μM bumetanide (△, ▲) at time zero. As shown, forskolin activates bumetanide-insensitive osmolyte efflux in shrunken cells with normal chloride content. Results from representative experiments are shown, but qualitatively similar results were observed in three experiments with each protocol.

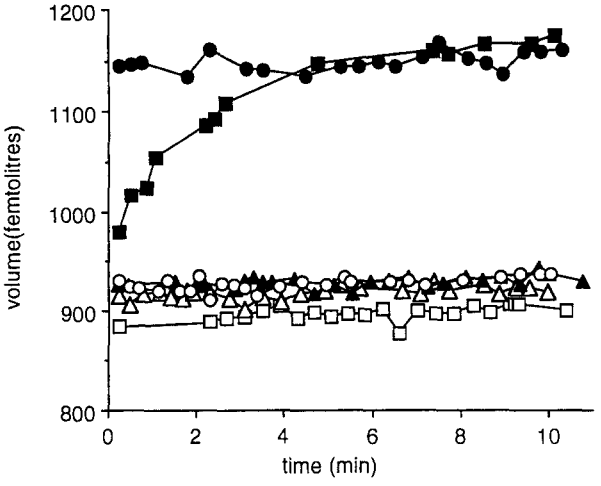

Fig. 11. Increasing cation permeability does not stimulate osmolyte uptake via the bumetanide-insensitive mechanism. Control cells were preincubated in chloride medium and maintained in chloride medium at time zero (●). All other cells were Cl^--depleted by 60 min preincubation in gluconate medium. Some chloride-depleted cells were maintained in gluconate medium at time zero (□), whereas others were exposed to chloride medium (■, ○, △, ▲). At time zero, some cells were additionally exposed to 2 μM gramicidin D (△), 10 μM valinomycin (▲), and/or 100 μM bumetanide (○, △, ▲). Results from a single experiment are shown, representative of results from four experiments.

cant forskolin-stimulated swelling was observed at later time points in the presence of a valinomycin voltage clamp. Results were corroborated by measurements of cellular Cl^- content made under the same gradient conditions. As shown in Fig. 14*A*, forskolin stimulates chloride uptake into cells incubated in potassium medium plus valinomycin and bumetanide. Figure 14*B* compiles four experiments performed under these conditions and compares the forskolin-stimulated chloride uptake into chloride-replete *vs.* chloride-depleted cells. As shown, chloride-depleted cells take up significantly less chloride at early time points. This suggests that activation of electrogenic chloride uptake is slow and time-dependent in chloride-depleted cells.

Discussion

In HT29 cells, CFTR expression and second messenger regulated chloride secretion are affected by epithelial polarization, cellular differentiation, and cell phenotype [30–33]. We studied net chloride transport activated by cAMP in a single HT29 subclone, to minimize confounding results by these variables. The HT29-C_1 subclone maintains a differentiated and polarized phenotype in culture [20] and has been suggested as a model for cells transitional between crypt and surface colonocytes, because it expresses apical Na^+/H^+ exchange [39] as well as high levels of CFTR mRNA [30]; proteins associated with both electroneutral sodium absorption and electrogenic chloride secretion [15].

Results demonstrate that cAMP activates (i) bumetanide-sensitive chloride uptake and (ii) bumetanide-insensitive chloride efflux in HT29-C_1 cells. The transport sensitive to loop diuretics (furosemide or bumetanide) is present in unstimulated cells and is restricted to the basolateral membrane. A bumetanide-sensitive basolateral Na/K/2Cl cotransporter has been shown to be activated by cAMP in HT29 and other epithelial cells [23, 26, 27]. The physiologic significance of this stim-

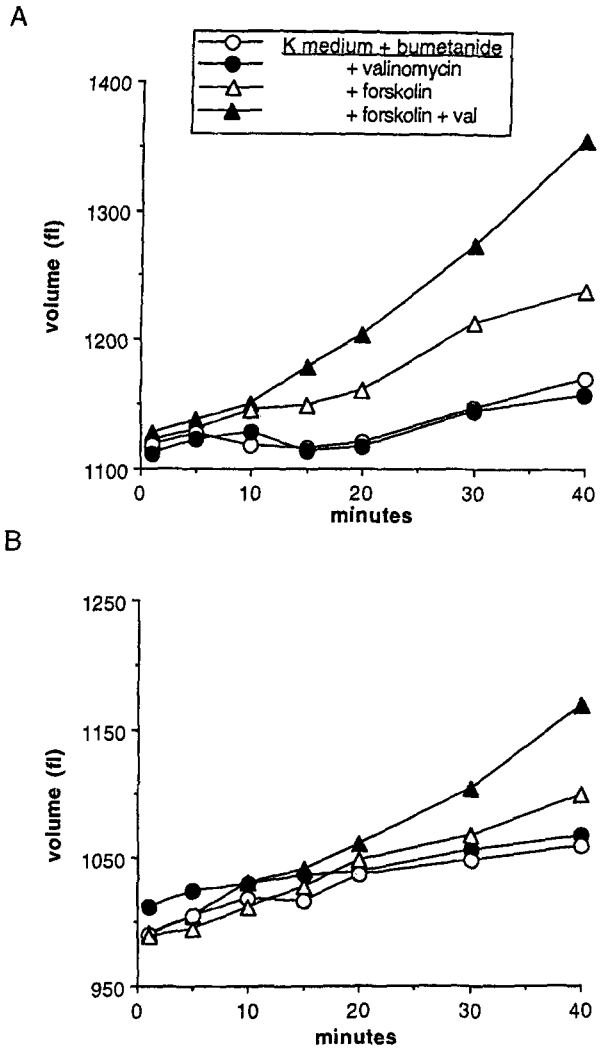

Fig. 12. Chloride depletion inhibits activation of an electrogenic uptake mechanism activated by cAMP. Cells were preincubated 60 min either in chloride medium (*A*) or gluconate medium (*B*). At time zero, all cells were exposed to 'KCl medium' (containing 130 mM KCl substituted for 130 mM NaCl in chloride medium) plus 100 μM bumetanide. Some cells were additionally exposed to 10 μM valinomycin (●), 10 μM forskolin (△), or both drugs (▲) at time zero. As shown, valinomycin stimulated osmolyte uptake in the presence of forskolin, but the ability of valinomycin to stimulate uptake was diminished in chloride-depleted cells. Results shown are from a single preparation, with qualitatively similar results observed in three experiments.

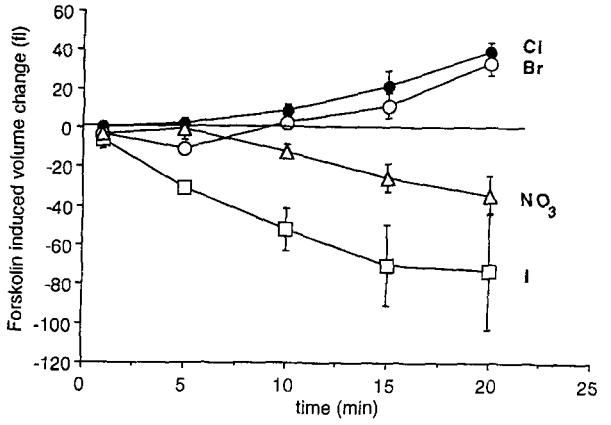

Fig. 13. The osmolyte uptake into depolarized cells discriminates between different extracellular anions. Cells preincubated in chloride medium were placed into medium containing 130 mM salt substituted for 130 mM NaCl in chloride medium. The salt was either KCl (●), KBr (○), KNO_3 (△), or KI (□). All media contained 100 μM bumetanide and 10 μM valinomycin to inhibit the cotransporter and clamp membrane potential. The figure compares the difference in cell volume at the indicated time points in the presence *vs.* absence of 10 μM forskolin. Forskolin-induced cell swelling (as observed in KCl medium in Fig. 12) is presented as a positive value. Results are mean ± SEM of four experiments.

ulation is to increase basolateral Cl^- uptake, and thereby sustain continued chloride secretion across the apical membrane. In this work we focused on the diuretic-insensitive chloride flux activated by cAMP. Results suggested that this pathway was present in the apical membrane and mediated chloride efflux in the presence of normal ion gradients.

The molecular identity of the electrogenic, bumetanide-insensitive, cAMP-stimulated chloride flux pathway can not be defined from our experiments. However, results suggest clear similarities and differences to known chloride channels. The flux mechanism mediates anion uptake with preference for $Cl^- \approx Br^- > NO_3^- > I^-$. An anion specificity for $Cl^- > I^-$ has been reported for a small conductance ohmic Cl^- channel observed in HT29-19A, T84, and Caco-2 colon carcinoma cells [5, 6, 8], as well as cells heterologously expressing wild-type CFTR [2, 3]. In HT29-19A, the conductivity series of this channel was further defined to be $Cl^- > NO_3^- > I^-$ [6]. The inwardly rectifying chloride channel ClC-2 has also been shown to conduct $Cl^- > I^-$ [41]. In contrast, outwardly rectifying conductances with a permeability series of I > Cl have been observed in a number of cell types (e.g., T_{84}, undifferentiated HT29 cells, airway epithelia) [25, 34, 47]. Based on perm-selectivity, the best candidates to explain our observations are ClC-2 and the ohmic chloride channel associated with CFTR. However, only the ohmic channel and some outward rectifying anion conductances have been shown to be activated by cAMP [5, 6, 8, 13, 16, 18, 25, 32, 44]. The observed ion selectivity and cAMP-activation of the electrogenic chloride flux in HT29-C_1 cells are most closely correlated with properties of the small-conductance ohmic channel, associated with CFTR.

Chloride-depleted cells were unable to promptly activate chloride uptake via the electrogenic cAMP-activated mechanism, even in the presence of depolarization and high K^+ permeability. Results were compared to the prompt activation of forskolin-sensitive chloride uptake when chloride replete cells were studied in the same extracellular medium. Measurements of in-

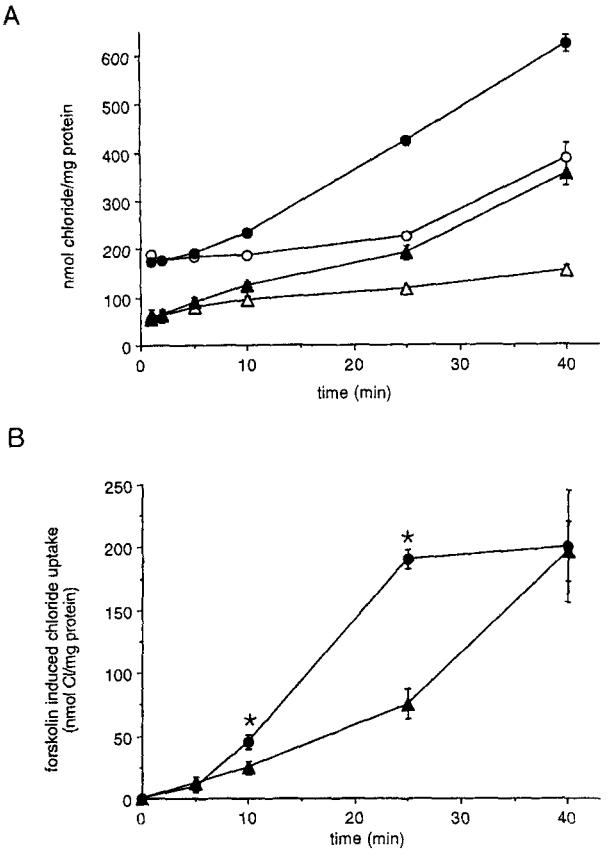

Fig. 14. Chloride depletion inhibits cAMP activation of chloride uptake into depolarized cells. Cells were preincubated 60 min either in chloride medium (○, ●) or gluconate medium (△, ▲). Results are mean ± SEM of 4–5 experiments. (*A*) At time zero, all cells were exposed to 'KCl medium' plus 100 μM bumetanide and 10 μM valinomycin. Some cells were additionally exposed to 10 μM forskolin (●, ▲) at time zero. As shown, forskolin stimulated bumetanide-insensitive chloride uptake, but the ability of forskolin to stimulate uptake was diminished in chloride-depleted cells. (*B*) The results in *A* are analyzed further. The figure compares the difference in cell chloride at the indicated time points in the presence *vs.* absence of 10 μM forskolin. Results are compiled separately for cells preincubated in chloride (●) *vs.* gluconate (▲) medium. The asterisk indicates statistical significance ($P < 0.02$) between conditions at the indicated time point. As shown, chloride depletion inhibits chloride uptake via the cAMP-stimulated, bumetanide-insensitive pathway.

tracellular Na^+, K^+ and Cl^- content suggest that the difference in results could not be explained by a decreased driving force for chloride uptake following chloride depletion. Chloride depletion causes a 39 mV increase in the chemical driving force for chloride reuptake (caused by the predicted fourfold drop in intracellular chloride concentration) which more than offsets the minor (−3 mV) decrease in electrical driving force caused by the 1.23-fold increase in cellular potassium concentration. Results suggest that depletion of cell chloride inhibits activation of cAMP-stimulated chloride flux, but that the inhibition is relieved slowly when cells are returned to chloride-containing media. Results from supporting experiments suggest that inhibition is not explained by limiting cation conductance, cell shrinkage, choice of substitute anion, or decreased generation of cAMP in chloride-depleted cells. Our results have interpretational limitations. It is possible that more than one chloride transport process is contained in the functional definition of "cAMP-stimulated and bumetanide-insensitive" fluxes. However all such processes would have to be similarly inhibited by chloride depletion. Alternatively, although effects of chloride depletion were observed in both suspended cells and cells attached to plastic, we did not perform a similar analysis with cells on filters (because we do not have adequate quantiative tools for such analyses). Therefore, it remains possible that chloride-depletion may not affect cells on filters.

Experiments suggest that some element distal to cAMP generation is required to activate electrogenic chloride flux. Results suggest that chloride-depletion is likely to either (i) enhance the action of an intrinsic inhibitory element or (ii) decrease the effect of an activating element. It has been shown that long chain fatty acids can act as blockers of chloride channels and may be intrinsic inhibitors [4, 24], but it is unknown whether the endogenous concentration of these substances in normal or chloride-depleted cells are inhibitory. One candidate for an activating factor is intracellular ATP, known to be required for activation of the small-conductance ohmic channel [1]. However, our experiments suggest that cellular ATP levels are adequate during chloride depletion to support normal cAMP generation and maintain normal Na^+ and K^+ gradients.

Another candidate activating factor is intracellular chloride ions. It has previously been proposed that intracellular chloride regulates the ohmic chloride channel, and a chloride channel in renal medullary membranes [44, 46]. Chloride could potentially act allosterically on the channels, via chloride-sensitive G-proteins [42], or via a chloride dependence for delivery of channel proteins to the apical membrane [11, 17, 33, 36]. In these cases, the time delay required for activation of cAMP-stimulated chloride uptake into chloride-depleted cells may be explained by the slow reentry of chloride via bumetanide-insensitive mechanisms (*see* Fig. 9*B*).

As discussed, the observed ion selectivity and cAMP-activation of the electrogenic chloride flux in HT29-C_1 cells are most closely correlated with properties of the small-conductance ohmic channel, associated with CFTR. Although it is known that CFTR is expressed in HT29-C_1 [31], the observed properties of the cAMP-activated flux in HT29-C_1 do not match those observed in CFTR expression systems. When CFTR is heterologously expressed in CHO or LTK^- cells [3, 44], a cAMP-activated outward chloride current (i.e., Cl^- uptake) has been observed under conditions of 11.8 mM or 10 mM intracellular Cl^-, respectively. In LTK- fibro-

blasts transfected with CFTR, raising intracellular chloride from 10 to 150 mM activated outward whole-cell currents in the absence of cAMP [44]. The effects of 150 mM Cl^- could not be fully explained by kinetic activation of the channel, since the relative activation by cAMP was reduced in high Cl^-. In comparison, our results demonstrate that chloride-depletion inhibits activation. Both results suggest a putative role for chloride in regulating channel function. We propose that in differentiated HT29-C_1 cells, chloride may interact with a (non-CFTR) protein to regulate function of the small-conductance ohmic channel. Results from heterologous expression systems and unpolarized HT29 cells suggest that this putative protein may not be expressed in all cell types [3, 44] and could be involved in CFTR trafficking [11, 33, 36]. Independent of mechanism, our results suggest that loss of cell chloride limits cAMP activation of an electrogenic chloride flux pathway. Such a mechanism would be beneficial to chloride secretory cells to limit the opening of apical chloride flux pathways when cellular chloride content is too low to support vectorial secretion.

The technical assistance of Dwight Derr is gratefully acknowledged. We also thank Dr. Chahrzad Montrose-Rafizadeh for help in performance of the chloride efflux experiments. This work was supported by National Institutes of Health grants RO1-DK42457 and PO1-DK44484.

References

1. Anderson, M.P., Berger, H.A., Rich, D.P., Gregory, R.J., Smith, A.E., Welsh, M.J. 1991. Nucleoside triphosphates are required to open the CFTR chloride channel. *Cell* **67:**775–784
2. Anderson, M.P., Gregory, R.J., Thompson, S., Souza, D.W., Paul, S., Mulligan, R.C., Smith, A.E., Welsh, M.J. 1991. Demonstration that the CFTR is a chloride channel by alteration of its anion selectivity. *Science* **253:**202–205
3. Anderson, M.P., Sheppard, D.N., Berger, H.A., Welsh, M.J. 1992. Chloride channels in the apical membrane of normal and cystic fibrosis airway and intestinal epithelia. *Am. J. Physiol.* **263:**L1–L14
4. Anderson, M.P., Welsh, M.J. 1990. Fatty acids inhibit apical membrane chloride channels in airway epithelia. *Proc. Natl. Acad. Sci.* **87:**7334–7338
5. Anderson, M.P., Welsh, M.J. 1991. Calcium and cAMP activate different chloride channels in the apical membrane of normal and cystic fibrosis epithelia. *Proc. Natl. Acad. Sci. USA* **88:**6003–6007
6. Bajnath, R.B., Groot, J.A., de Jonge, H.R., Kansen, M., Bijman, J. 1993. Synergistic activation of nonrectifying small conductance chloride channels by forskolin and phorbol esters in cell-attached patches of the human colon carcinoma cell line HT-29cl.19A. *Pfluegers Arch.* **425:**100–108
7. Bear, C.E., Li, C., Kartner, N., Bridges, R., Jensen, T., Ramjeesingh, M., Riordan, J.R. 1992. Purification and functional reconstitution of the cystic fibrosis transmembrane conductance regulator (CFTR). *Cell* **68:**809–818
8. Bear, C.E., Reyes, E.F. 1992. cAMP activated chloride conductance in the colonic cell line, Caco-2. *Am. J. Physiol.* **262:**C251–C256
9. Berger, H.A., Travis, S.M., Welsh, M.J. 1993. Regulation of the cystic fibrosis transmembrane conductance regulatory Cl^- channel by specific protein kinases and protein phosphatases. *J. Biol. Chem.* **268:**2037–2047
10. Berschneider, H.M., Knowles, M.R., Asiskhan, R.G., Boucher, R.C., Tobey, N.A., Orlando, R.C., Powell, D.W. 1988. Altered intestinal chloride transport in cystic fibrosis. *FASEB J.* **2:**2625–2629
11. Bradbury, N.A., Bridges, R.J. 1994. Role of membrane trafficking in plasma membrane solute transport. *Am. J. Physiol.* **267:**C1–C24
12. Bradford, M.M. 1976. A rapid and sensitive method for the quantitation of microgram quantities of protein utilizing the principle of protein-dye binding. *Anal. Biochem.* **72:**248–254
13. Cliff, W.H., Frizzell, R.A. 1990. Separate Cl^- conductances activated by cAMP and Ca^{2+} in Cl^--secreting epithelial cells. *Proc. Natl. Acad. Sci. USA* **87:**4956–4960
14. Dechecchi, M.C., Tamanini, A., Berton, G., Cabrini, G. 1993. Protein kinase C activates chloride conductance in C127 cells stably expressing the cystic fibrosis gene. *J. Biol. Chem.* **268(15):**11321–11325
15. Donowitz, M., Welsh, M.J. 1987. Regulation of mammalian small intestinal electrolyte secretion. *In:* Physiology of the Gastrointestinal tract. 2nd edition. L.R. Johnson, editor, pp. 1351–1388, Raven, New York
16. Egan, M., Flotte, T., Aflone, S., Solow, R., Zeitlin, P.L., Carter, B.J., Guggino, W.B. 1992. Defective regulation of outwardly rectifying Cl^- channels by protein kinase A corrected by insertion of CFTR. *Nature* **358:**581–584
17. Fittschen, C. Henson, P.M. 1994. Linkage of Azurophil granule secretion in neutrophils to chloride ion transport and endosomal transcytosis. *J. Clin. Invest.* **93:**247–255
18. Gabriel, S.E., Clarke, L.L., Boucher, R.C., Stutts, M.J. 1993. CFTR and outward rectifying chloride channels are distinct proteins with a regulatory relationship. *Nature* **363:**263–268
19. Hardcastle, J., Hardcastle, P.T., Taylor, C.J., Goldhill, J. 1991. Failure of cholinergic stimulation to induce a secretory response from the rectal mucosa in cystic fibrosis. *Gut* **32:**1035–1039
20. Huet, C., Sahuquillo-Marino, C., Coudrier, E., Louvard, D. 1987. Absorptive and mucus-secreting subclones isolated from a multipotent intestinal cell line (HT29) provide new models for cell polarity and terminal differentiation. *J. Cell Biol.* **105:**345–357
21. Illsley, N.P., Verkman, A.S. 1987. Membrane chloride transport measured using a chloride-sensitive fluorescent probe. *Biochemistry* **26:**1215–1219
22. Jefferson, D.M., Valentich, J.D., Marini, F.C., Grubman, S.A., Iannuzzi, M.C., Dorkin, H.L., Li, M., Klinger, K.W., Welsh, M.J. 1990. Expression of normal and cystic fibrosis phenotypes by continuous airway epithelial cell lines. *Am. J. Physiol.* **259:**L496–L505
23. Kim, H.D., Tsai, Y.-S., Franklin, C.C., Turner, J.T. 1988. Characterization of $Na^+/K^+/2Cl^-$ cotransport in cultured HT29 human colonic adenocarcinoma cells. *Biochim. Biophys. Acta* **946:**397–404
24. Kunzelmann, K., Tilmann, M., Hansen, Ch.P., Greger, R. 1991. Inhibition of epithelial chloride channels by cytosol. *Pfleugers Arch.* **418:**479–490
25. Li, M., McCann, J.D., Welsh, M.J. 1990. Apical membrane Cl^- channels in airway epithelia: anion selectivity and effect of an inhibitor. *Am. J. Physiol.* **259:**C295–C301
26. Liedtke, C.M. 1989. Alpha-adrenergic regulation of Na-Cl cotransport in human airway epithelium. *Am. J. Physiol.* **257:**L125–L129
27. Lytle, C., Forbush III, B. 1992. The Na-K-Cl cotransporter protein of shark rectal gland. II. regulation by direct phosphorylation. *J. Biol. Chem.* **267:**25438–25443

28. Matthews, J.B., Smith, J.A., Tally, K.J., Awtrey, C.S., Nguyen, H., Rich, J., Madara, J.L. 1994. Na-K-2Cl cotransport in intestinal epithelial cells: influence of chloride efflux and F-actin on regulation of cotransporter activity and bumetanide binding. *J. Biol. Chem.* **269:**15703–15709
29. Montrose, M.H., Friedrich, T., Murer, H. 1987. Measurements of intracellular pH in single LLC-PK_1 cells: recovery from an acid load via basolateral Na^+/H^+ exchange. *J. Membrane Biol.* **97:**63–78
30. Montrose-Rafizadeh, C., Blackmon, D.L., Hamosh, A., Oliva, M.M., Hawkins, A.L., Curristin, S.M., Griffin, C.A., Yang, V.W., Guggino, W.B., Cutting, G.R., Montrose, M.H. 1992. Regulation of CFTR gene transcription and alternative RNA splicing in a model of developing intestinal epithelium. *J. Biol. Chem.* **267:**19299–19305
31. Montrose-Rafizadeh, C., Guggino, W.B., Montrose, M.H. 1991. Cellular differentiation regulates expression of Cl^- transport and cystic fibrosis transmembrane conductance regulator mRNA in human intestinal cells. *J. Biol. Chem.* **266:**4495–4499
32. Morris, A.P., Cunningham, S.A., Benos, D.J., Frizzell, R.A. 1992. Cellular differentiation is required for cAMP but not Ca^{2+}-dependent Cl^- secretion in colonic epithelial cells expressing high levels of cystic fibrosis transmembrane conductance regulator. *J. Biol. Chem.* **267:**5575–5583
33. Morris, A.P., Cunningham, S.A., Tousson, A., Benos, D.J., Frizzell, R.A. 1994. Polarization-dependent apical membrane CFTR targetting underlies cAMP-dependent Cl^- secretion in epithelial cells. *Am. J. Physiol.* **266:**C254–C268
34. Morris, A.P., Frizzell, R.A. 1993. Ca^{2+}-dependent Cl^- channels in undifferentiated human colonic cells (HT-29). II. regulation and rundown. *Am. J. Physiol.* **264:**C977–C985
35. O'Loughlin, E.V., Hunt, D.M., Gaskin, K.J., Stiel, D., Bruzuszcak, I.M., Martin, H.C., Bambach, C., Smith, R. 1991. Abnormal epithelial transport in cystic fibrosis jejunum. *Am. J. Physiol.* **260:**G758–G763
36. Prince, L.S., Workman, R.B. Jr., Marchase, R.B. 1994. Rapid endocytosis of the cystic fibrosis transmembrane conductance regulator chloride channel. *Proc. Natl. Acad. Sci.* **91:**5192–5196
37. Robertson, M.A., Foskett, J.K. 1994. Na transport pathways in secretory acinar cells: membrane cross talk mediated by $[Cl]_i$. *Am. J. Physiol.* **267:**C146–C156
38. Rowe, W.A., Blackmon, D.L., Montrose, M.H. 1993. Propionate activates multiple ion transport mechanism in the HT29-18-C1 human colon cell line. *Am. J. Physiol.* **265:**G564–G571
39. Rowe, W.A., Lesho, M.J., Montrose, M.H. 1994. Polarized Na/H exchange function is pliable in response to transepithelial gradients of propionate. *Proc. Natl. Acad. Sci.* **91:**6166–6170
40. Solc, C.K., Wine, J.J. 1991. Swelling-induced and depolarization-induced Cl^- channels in normal and cystic fibrosis epithelial cells. *Am. J. Physiol.* **261:**C658–C674
41. Thiemann, A., Gründer, S., Pusch, M., Jentsch, T.J. 1992. A chloride channel widely expressed in epithelial and nonepithelial cells. *Nature* **356:**57–60.
42. Tilly, B.C., Kansen, M., Van Gageldonk, P.G., van den Berghe, N., Galjaard, H., Bijman, J., deJonge, H.R. 1991. G-proteins mediate intestinal chloride channel activation. *J. Biol. Chem.* **266:**2036–2040
43. Wagoner, K., Pallotta, B.S. 1988. Modulation of acetylcholine receptor desensitization by forskolin is independent of cAMP. *Science* **240:**1655–1657
44. Wang, X., Marunaka, Y., Fedorko, L., Dho, S., Foskett, J.K., O'Brodovich, H. 1993. Activation of Cl^- currents by intracellular chloride in fibroblasts stably expressing the human cystic fibrosis transmembrane conductance regulator. *Can. J. Physiol. Pharmacol.* **71:**645–649
45. Willumsen, N.J., Boucher, R.C. 1989. Activation of an apical Cl^- conductance by calcium ionophores in cystic fibrosis airway epithelia. *Am. J. Physiol.* **256:**C226–C233
46. Winters, C.J., Reeves, W.B., Andreoli, T.E. 1990. Cl^- channels in basolateral renal medullary membranes: Determinants of single-channel activity. *J. Membrane Biol.* **118:**269–278
47. Worrell, R.T., Butt, A.G., Cliff, W.H., Frizzell, R.A. 1989. A volume-sensitive chloride conductance in human colonic cell line T84. *Am. J. Physiol.* **256:**C1111–C1119